Contents

This supplement contains the microphysical parameter plots of Fig. 3a–c of the main article, but retrieved using different radar band combinations. The mass-weighted mean diameter is shown in Figs. S1–S7, the bulk density in Figs. S8–S14, and the ice water content in Figs. S15–S21. The prior sensitivity analysis of Fig. 6 of the main article is also shown in Figs. S22–S28 using different band combinations.

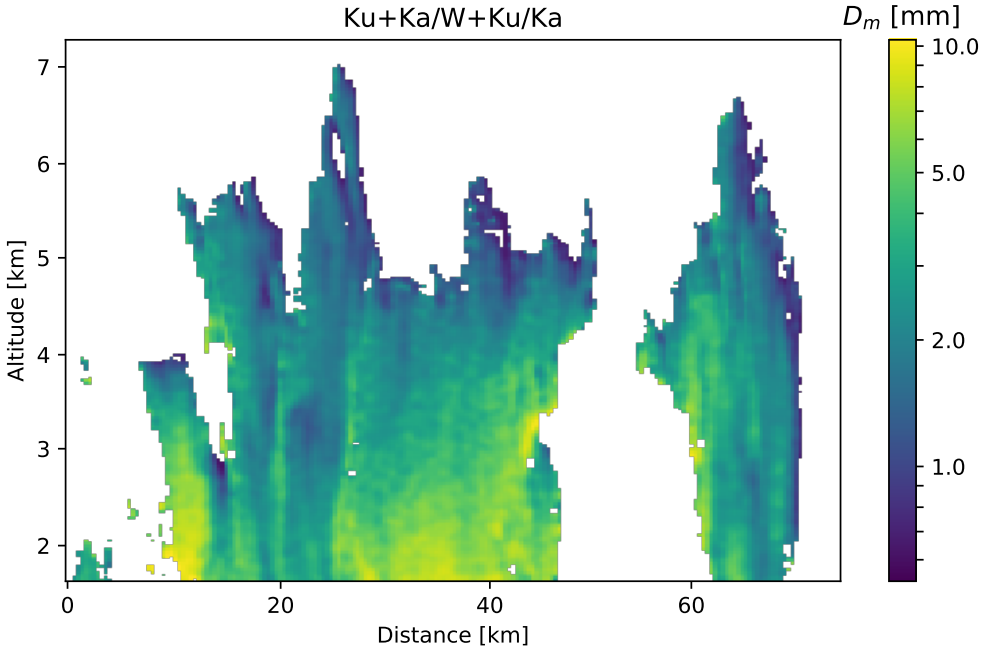

Figure S1. The mass-weighted mean diameter for the December 4, 2015 case, retrieved using the Ku-band reflectivity, the Ka/W band dual-wavelength ratio (DWR) and the Ku/Ka-band DWR. This plot is equivalent to Fig. 3a of the main article, but the colors have been rescaled in order to retain consistency between Figs. S1–S7.

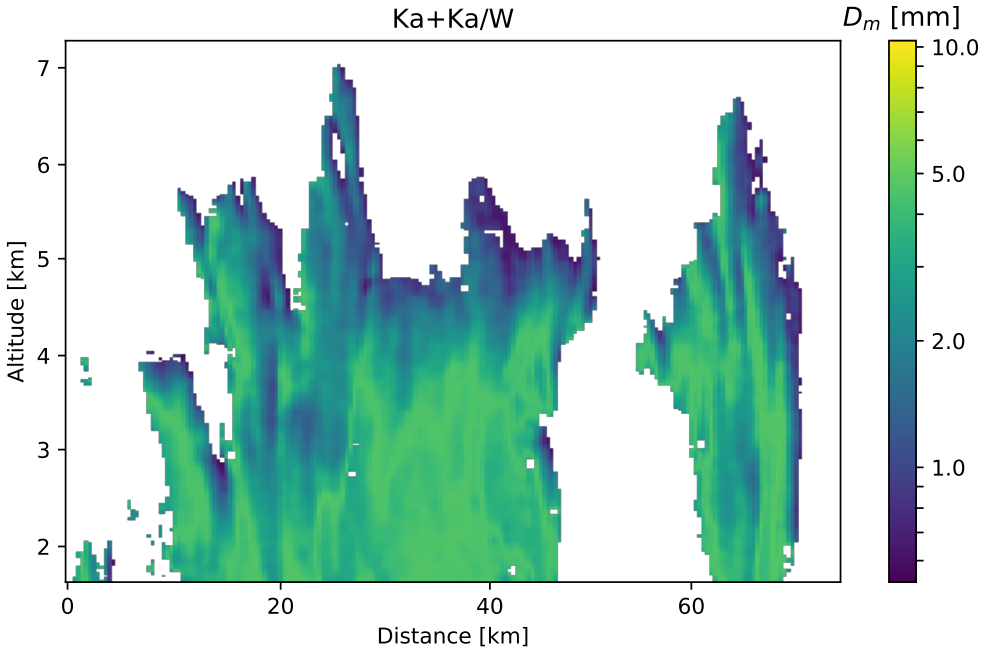

Figure S2. As Fig. S1, but retrieved using the Ka-band reflectivity and the Ka/W band DWR.

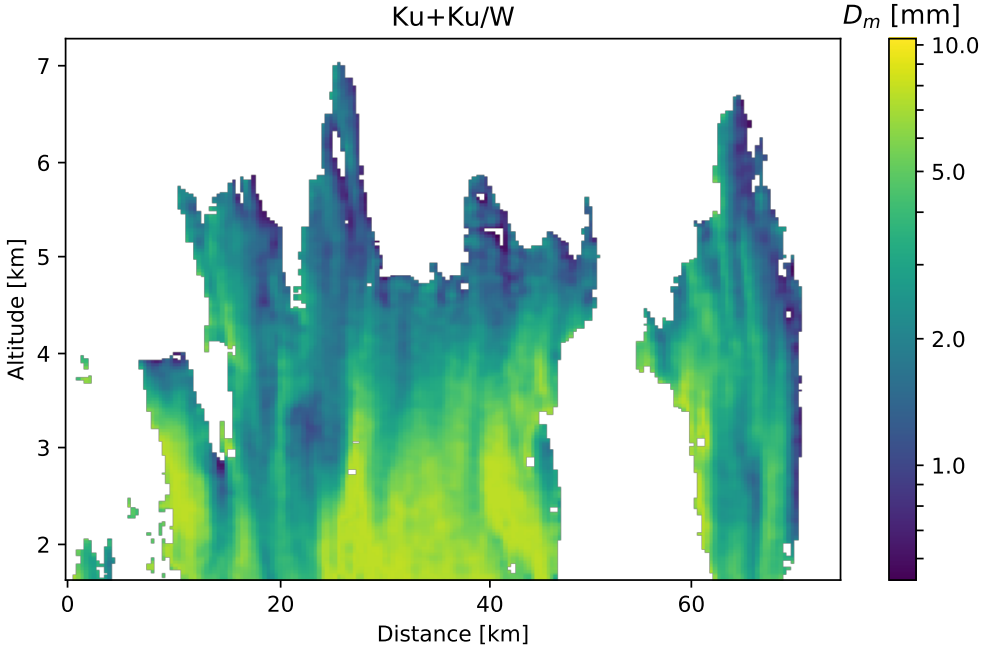

Figure S3. As Fig. S1, but retrieved using the Ku-band reflectivity and the Ku/W band DWR.

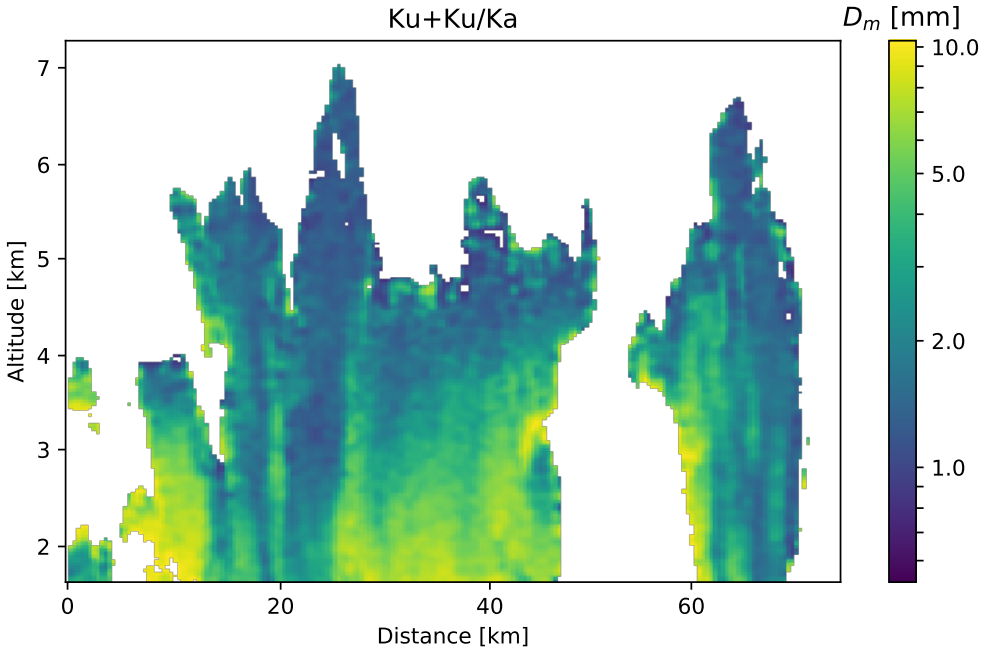

Figure S4. As Fig. S1, but retrieved using the Ku-band reflectivity and the Ku/Ka band DWR.

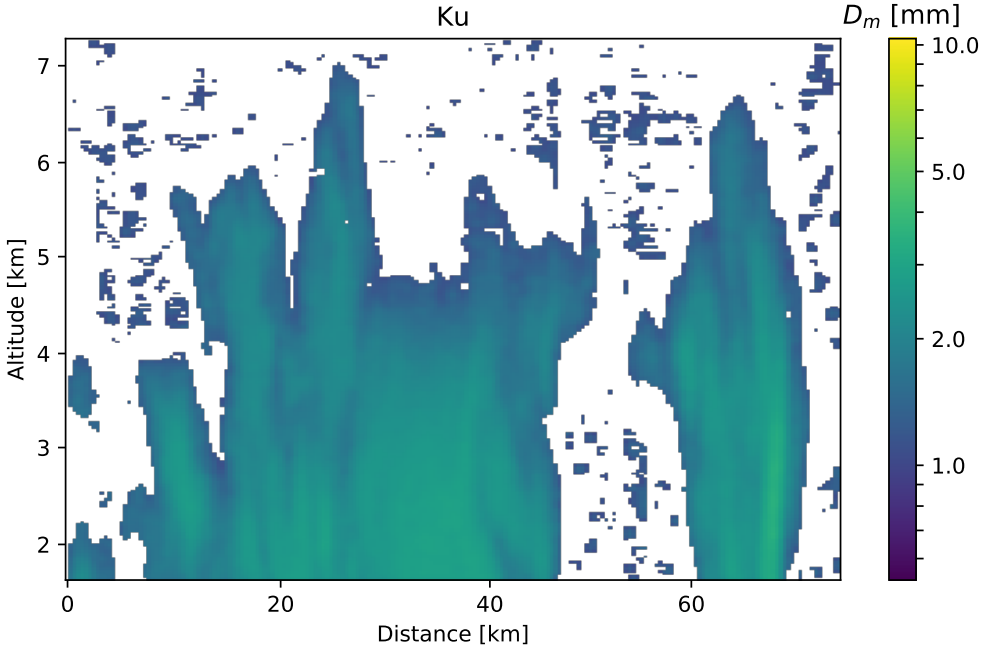

Figure S5. As Fig. S1, but retrieved using the Ku-band reflectivity only.

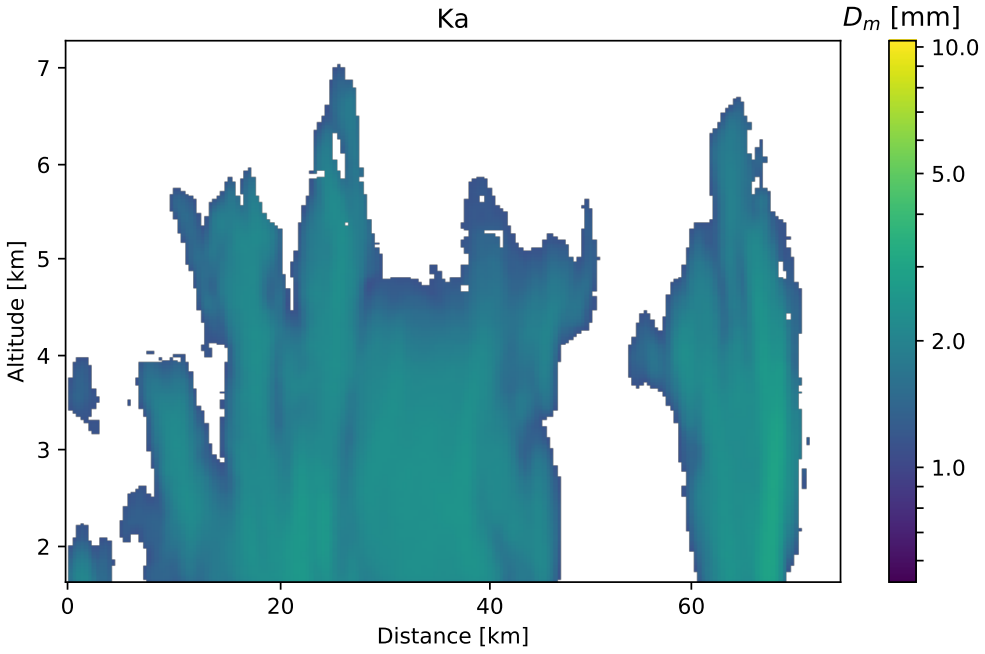

Figure S6. As Fig. S1, but retrieved using the Ka-band reflectivity only.

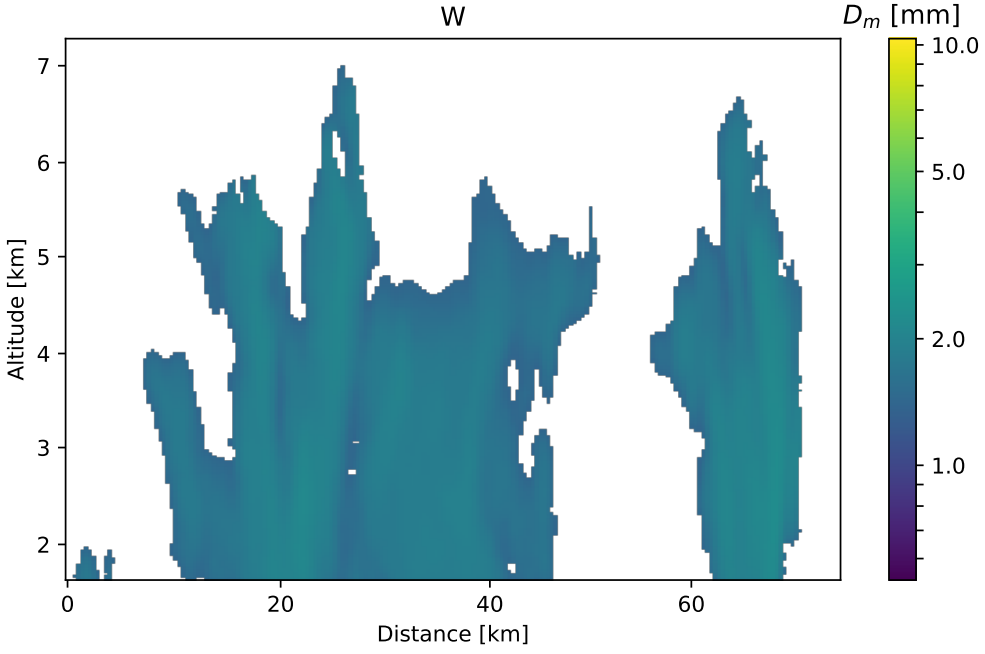

Figure S7. As Fig. S1, but retrieved using the W-band reflectivity only.

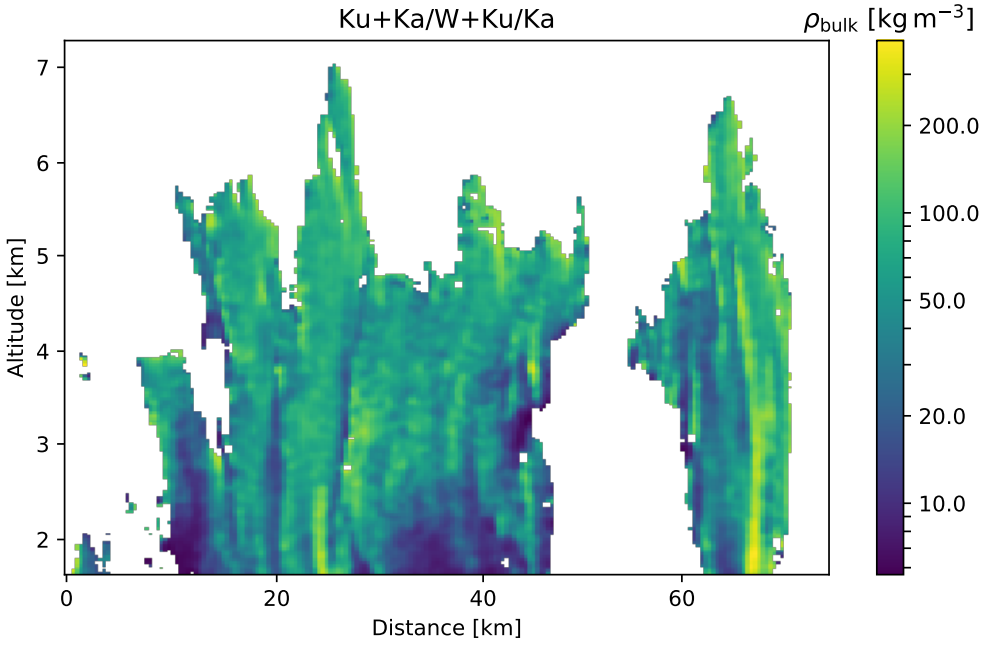

Figure S8. The bulk density for the December 4, 2015 case, retrieved using the Ku-band reflectivity, the Ka/W band dual-wavelength ratio (DWR) and the Ku/Ka-band DWR. This plot is equivalent to Fig. 3b of the main article, but the colors have been rescaled in order to retain consistency between Figs. S8–S14.

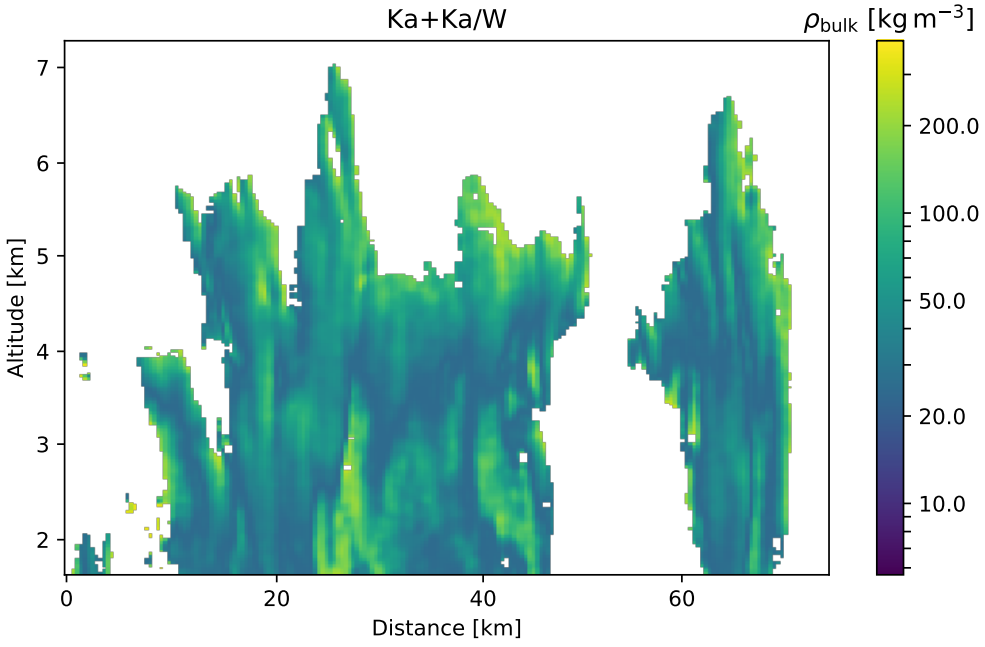

Figure S9. As Fig. S8, but retrieved using the Ka-band reflectivity and the Ka/W band DWR.

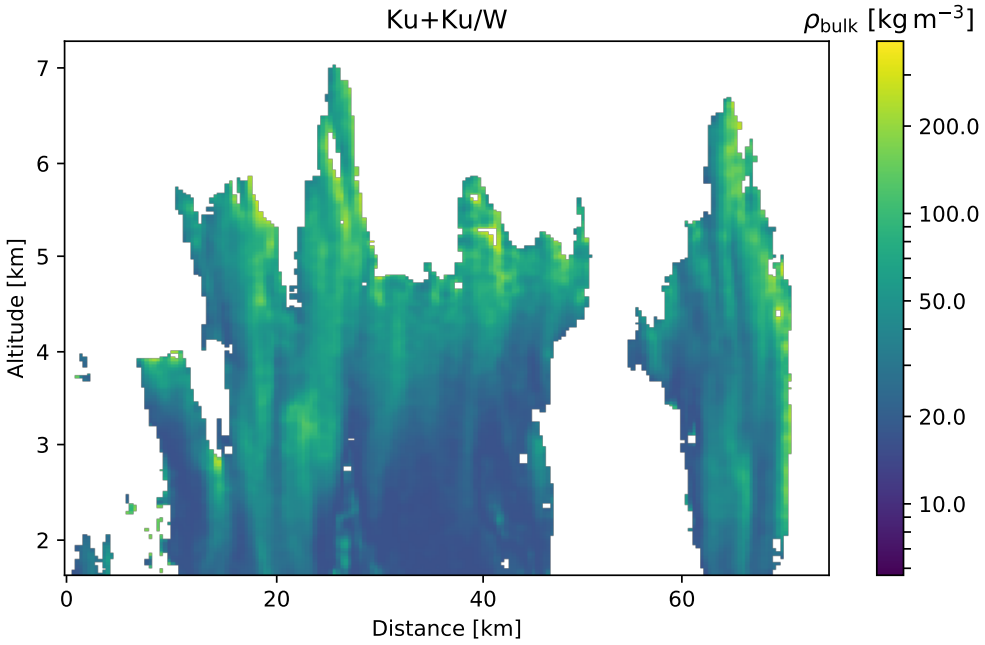

Figure S10. As Fig. S8, but retrieved using the Ku-band reflectivity and the Ku/W band DWR.

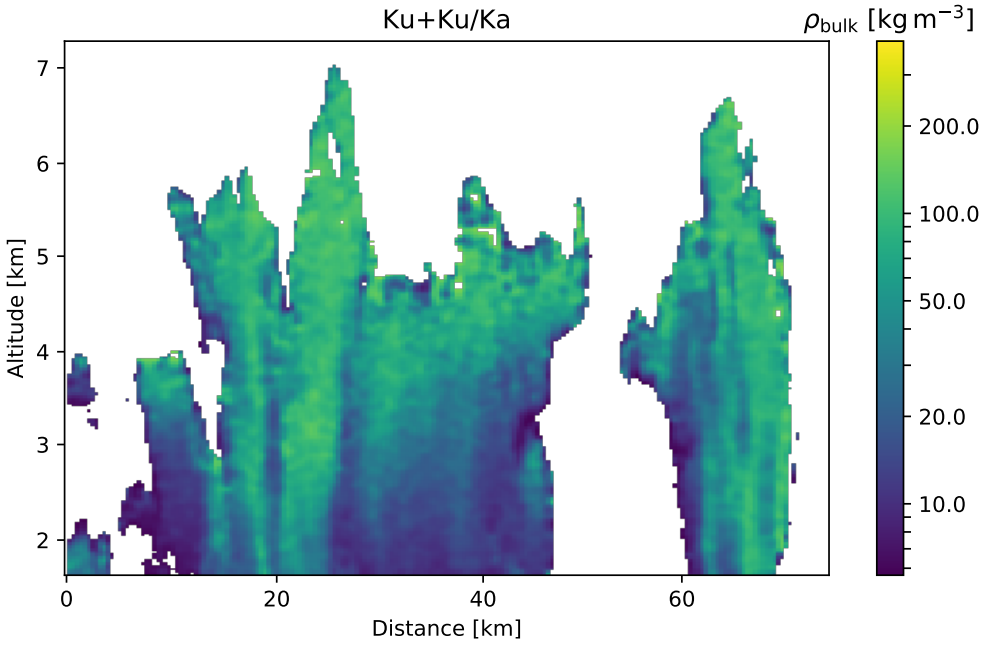

Figure S11. As Fig. S8, but retrieved using the Ku-band reflectivity and the Ku/Ka band DWR.

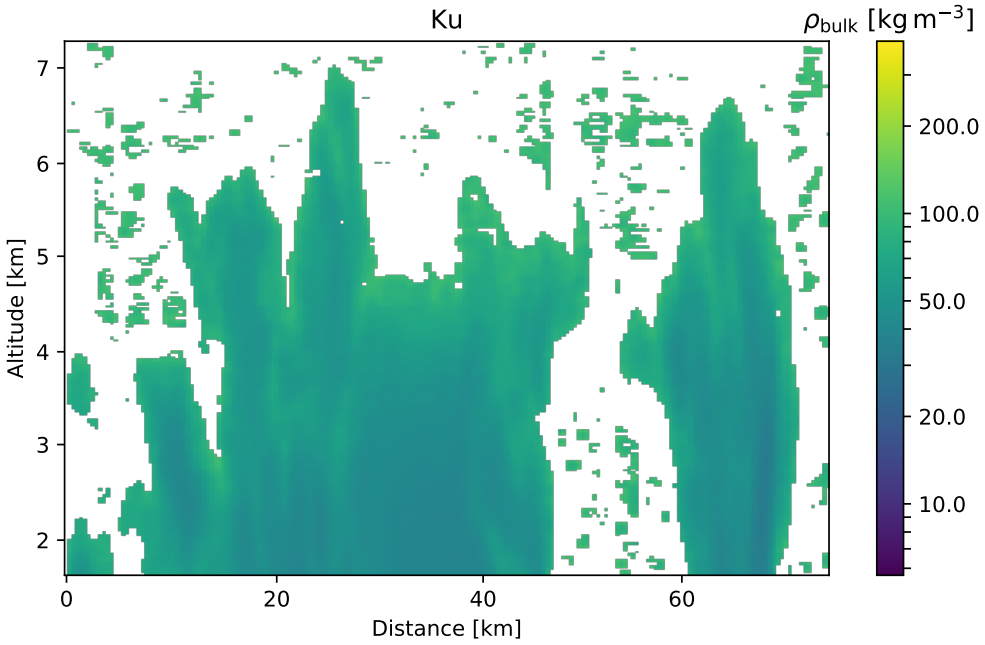

Figure S12. As Fig. S8, but retrieved using the Ku-band reflectivity only.

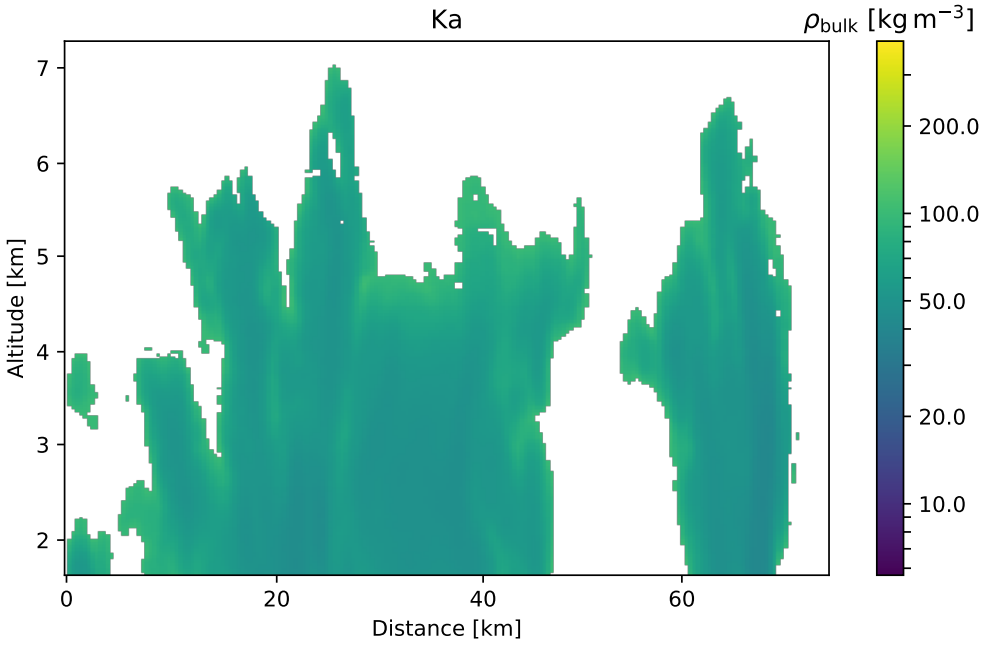

Figure S13. As Fig. S8, but retrieved using the Ka-band reflectivity only.

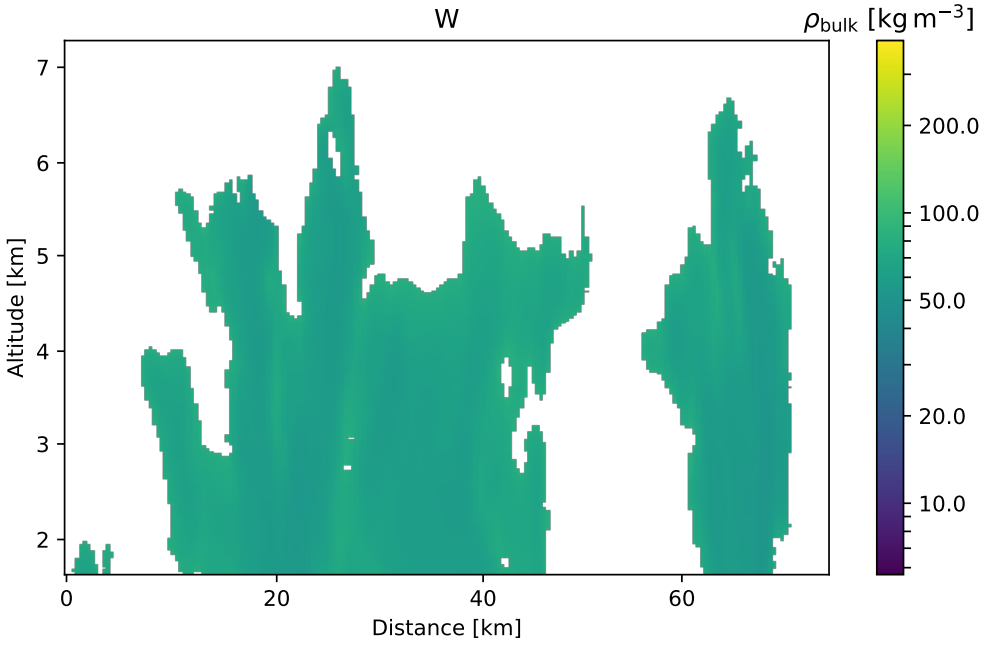

Figure S14. As Fig. S8, but retrieved using the W-band reflectivity only.

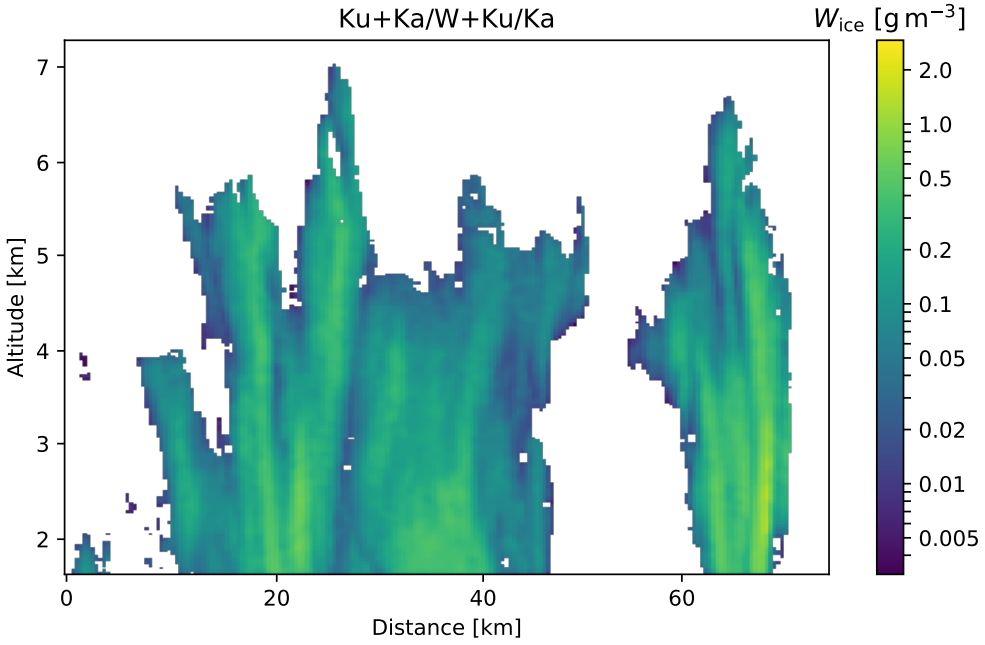

Figure S15. The ice water content for the December 4, 2015 case, retrieved using the Ku-band reflectivity, the Ka/W band dual-wavelength ratio (DWR) and the Ku/Ka-band DWR. This plot is equivalent to Fig. 3c of the main article, but the colors have been rescaled in order to retain consistency between Figs. S15–S21.

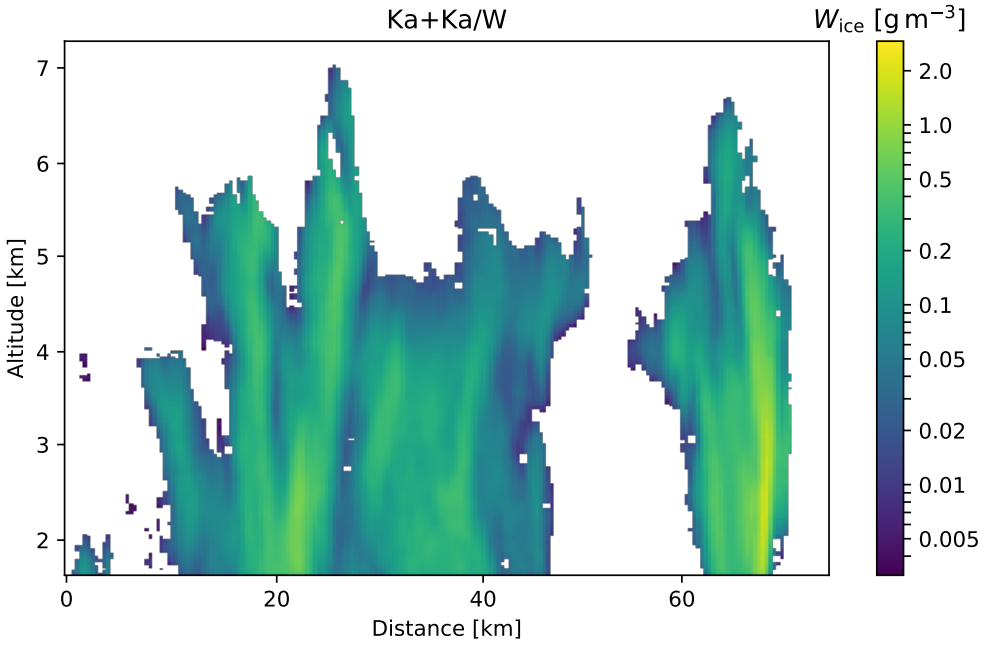

Figure S16. As Fig. S15, but retrieved using the Ka-band reflectivity and the Ka/W band DWR.

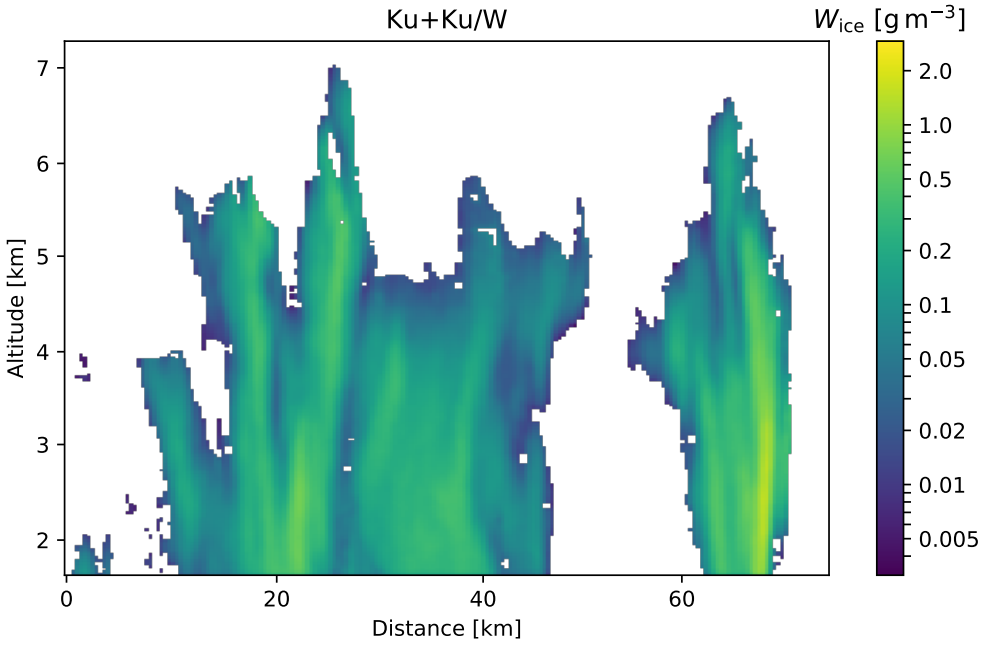

Figure S17. As Fig. S15, but retrieved using the Ku-band reflectivity and the Ku/W band DWR.

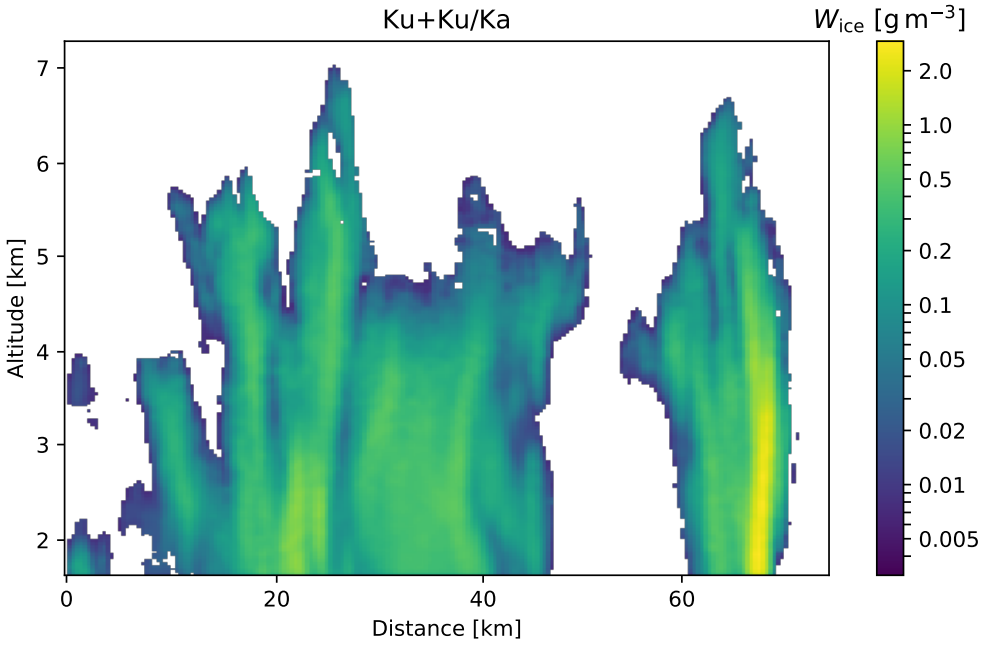

Figure S18. As Fig. S15, but retrieved using the Ku-band reflectivity and the Ku/Ka band DWR.

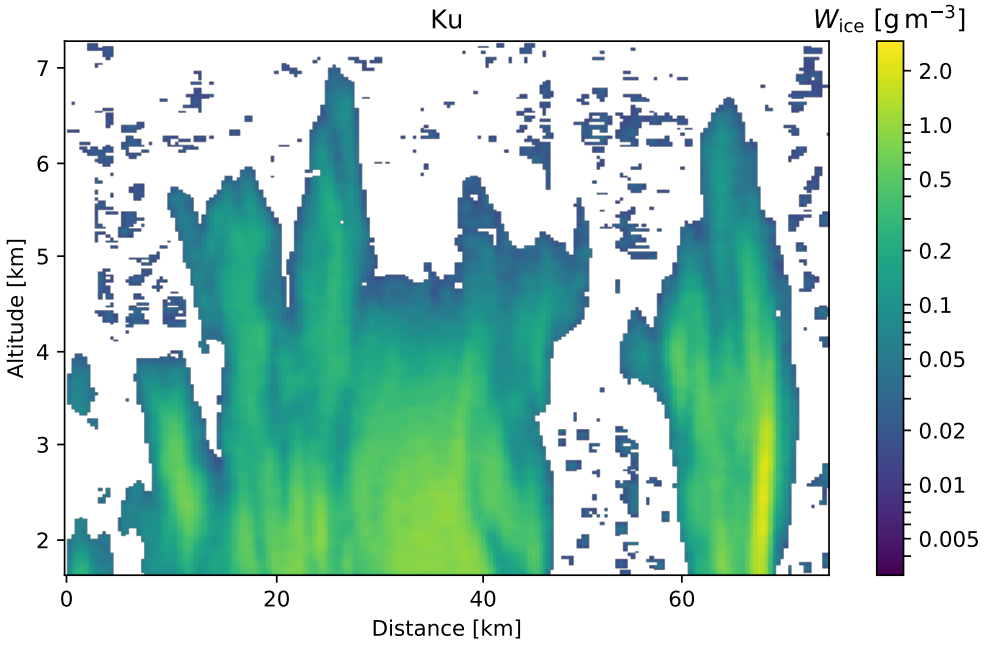

Figure S19. As Fig. S15, but retrieved using the Ku-band reflectivity only.

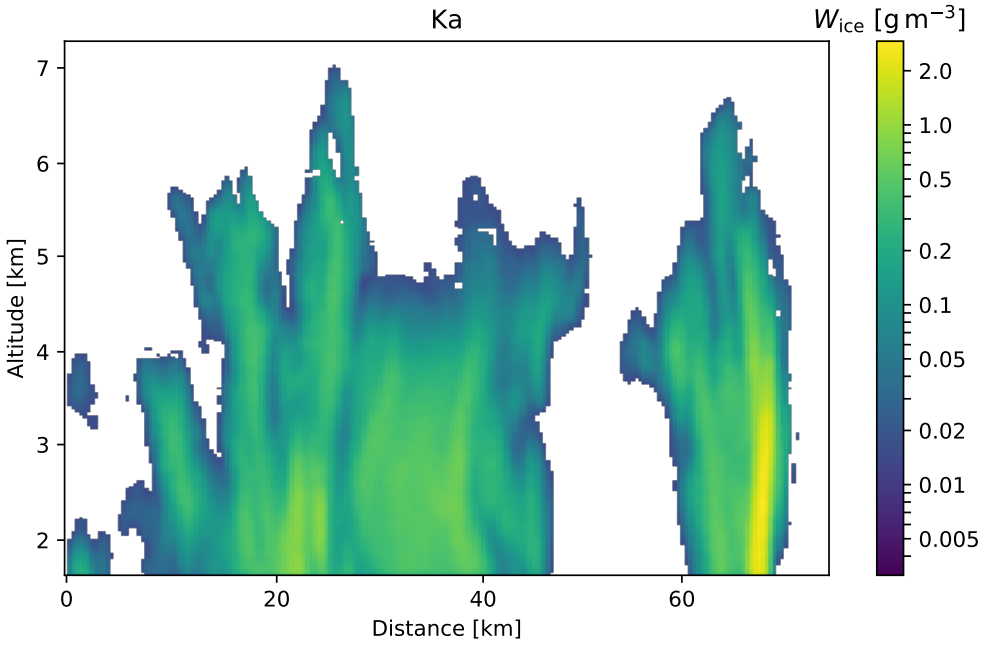

Figure S20. As Fig. S15, but retrieved using the Ka-band reflectivity only.

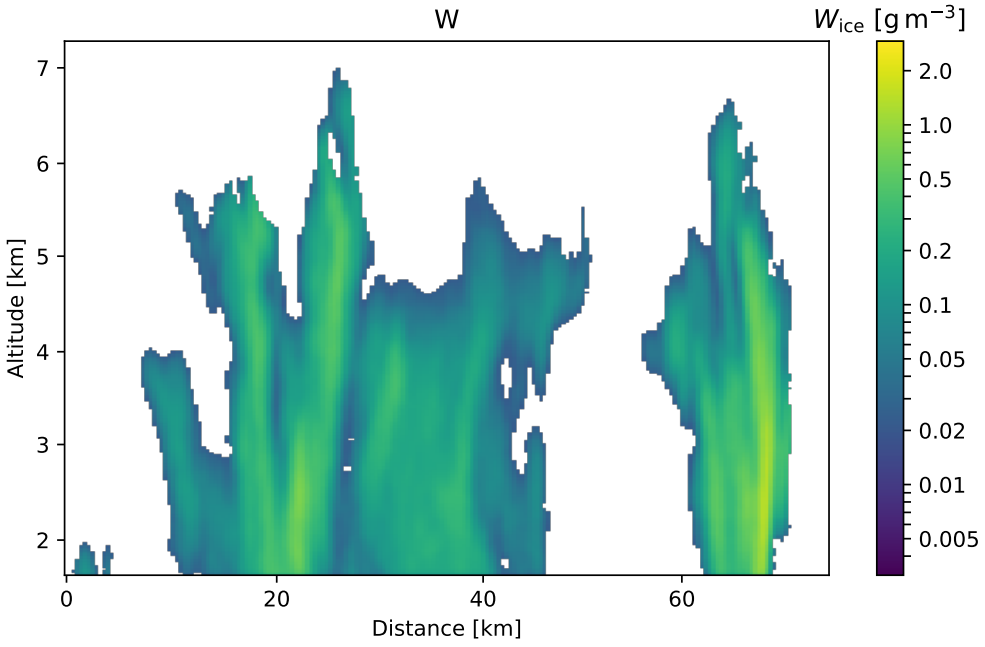

Figure S21. As Fig. S15, but retrieved using the W-band reflectivity only.

Figure S22. This is equivalent to the prior sensitivity study of Fig. 6 of the main article, but the colors have been rescaled for consistency between Figs. S22–S28.

Figure S23. As Fig. S22, but retrieved using the Ka-band reflectivity and the Ka/W band DWR.

Figure S24. As Fig. S22, but retrieved using the Ku-band reflectivity and the Ku/W band DWR.

Figure S25. As Fig. S22, but retrieved using the Ku-band reflectivity and the Ku/Ka band DWR.

Figure S26. As Fig. S22, but retrieved using the Ku-band reflectivity only.

Figure S27. As Fig. S22, but retrieved using the Ka-band reflectivity only.

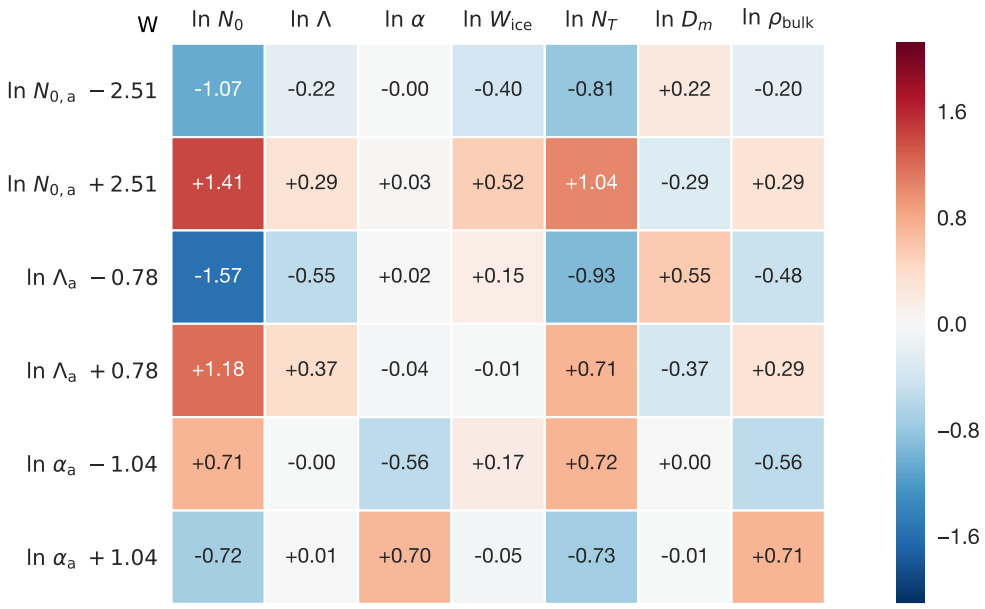

Figure S28. As Fig. S22, but retrieved using the W-band reflectivity only.